J Forensic Sci, November 2008, Vol. 53, No. 6
doi: 10.1111/j.1556-4029.2008.00860.x
Available online at: www.blackwell-synergy.com

John W. Bond,[1] *D.Phil.*

The Thermodynamics of Latent Fingerprint Corrosion of Metal Elements and Alloys

ABSTRACT: Redox reactions taking place between the surface of a metal and fingerprint residue have been expressed thermodynamically in terms of both the Nernst equation for reduction potential and the complexation constant for the formation of complex metal halide ions in aqueous solution. These expressions are used to explain experimental results for the corrosion of 10 different metal elements by fingerprint residue in air at room temperature. Corrosion of noble metals, such as silver and gold, supports the proposition that the degree of metal corrosion is enhanced by the presence of chloride ions in eccrine sweat. Extending the experiments to include 10 metal alloys enabled the construction of a fingerprint corrosion series for 20 different metals. Fingerprint corrosion on metals alloyed with > ~40% copper was found to display third level fingerprint detail. A comparison of both conventional ink on paper and digital (Livescan) fingerprinting techniques with fingerprints deposited on 9 Karat gold alloy has shown that gold alloy depositions are least susceptible to third level detail obliteration by poor fingerprint capturing techniques.

KEYWORDS: forensic science, latent fingerprint, print visualization, metal surface

The discoloration of a metal surface through exposure to oxidizing agents is well known, as is the wearing away of metal through corrosion (1). The ability of some metal elements and alloys to resist corrosion and the principles of dissimilar metal corrosion form the basis of metal corrosion theory, which is used in practice to prevent unwanted corrosion.

When latent fingerprints are deposited on metal surfaces, recent research has focused on fingerprint visualization techniques that exploit the chemical reaction that can occur between the metal surface and the fingerprint residue. This reaction, effectively a corrosion of the metal surface, results in a change to both the chemical and physical characteristics of the metal surface. The use of such techniques requires no physical or chemical development of the fingerprint prior to visualization unlike conventional treatments, such as powdering, cyanoacrylate fuming, suspension in small particle reagents (2–4), or electrochemical etching (5–8).

Williams et al. have demonstrated fingerprint visualization on metals using a Scanning Kelvin Microprobe (9,10). This technique is based on a measurement of the potential difference arising between a wire probe and the metal surface due to differences in their respective work functions. The magnitude of this potential difference is affected by fingerprint residue corrosion of the metal surface. By measuring this variation in potential, an image of the fingerprint has been visualized in terms of potential difference. The usefulness of this technique was demonstrated by visualizing fingerprints deposited beneath layers of soot or paint and also on brass cartridge cases where fingerprints were deposited postfiring.

More recently, we have considered the corrosion of brass, copper, mild steel, and aluminum substrates by fingerprint residue (11). Heating the metal to several hundred degrees celsius produced durable images of fingerprints deposited on brass, copper, and mild steel and we demonstrated how this might be used to enable fingerprint visualization after the metal had been subject to smoke and soot contamination or spray painting. We also showed how fingerprints deposited on brass cartridge cases prefiring could be visualized postfiring by the application of an electrostatic charge and conducting powder to the cartridge cases. Similar durable images were found to occur by leaving fingerprint deposits on metal in air at room temperature for several days. We highlighted the variation in both the ability of an individual's fingerprint residue to corrode metal and the degree of corrosion on different metals. We postulated, in keeping with corrosion science, that this was due to both the variable composition of eccrine sweat and the amount of sweat secreted by individuals (12).

In this paper, we examine further fingerprint visualization on metals by conducting experiments with 10 different metal elements and observing the degree of corrosion caused by fingerprint residue on each element. We demonstrate how variations in the degree of corrosion between elements can be explained thermodynamically in terms of the Nernst equation with calculated values for the standard reduction potential and complexation constant used to explain the experimental results.

We then extend the range of metals being examined by including 10 different metal alloys and, together with the 10 metal elements, produce a fingerprint corrosion series that orders these metals by the ease with which fingerprints can produce durable corroded images on the metal surface. Finally, we show that the ease of visualization of fingerprint residue corrosion on metal alloys is dependent on the alloying elements and demonstrate how the corrosion can be less susceptible to the obliteration of third level fingerprint detail than either conventional ink on paper or digital fingerprinting techniques.

Theory

The following is a summary of reduction potential, its derivation and how it gives a measure of the tendency for chemical species present in aqueous solution (such as metal ions or molecules) to gain electrons (i.e., be reduced). A more detailed discussion of reduction potential can be found in, for example, Landolt (13) or Trethewey and Chamberlain (14).

The readiness of a metal to participate in a reaction that can lead to its corrosion can be expressed in terms of the Gibbs free energy

[1]Scientific Support Unit, Northamptonshire Police, Wootton Hall, Northampton NN4 0JQ, U.K.

Received 14 Nov. 2007; and in revised form 16 Feb. 2008; accepted 8 Mar. 2008.

of reaction (G) and the net change in this energy during a reaction (ΔG). For systems in equilibrium, there is no net change in free energy and, therefore, $\Delta G = 0$. Spontaneous reactions are associated with a decrease in the free energy, that is, $\Delta G < 0$ and values for ΔG may be expressed in terms of the activity of species present in a given reaction. Consider the reaction

$$0 = \sum \upsilon_i B_i \tag{1}$$

in which υ_i represents the stoichiometric coefficient of the species B_i present in the reaction. By definition, values of υ_i for the reaction products are positive and for the reactants negative.

ΔG can be expressed as

$$\Delta G = \Delta G^0 + RT \ln K \tag{2}$$

where ΔG^0 represents the standard free energy of reaction (under standard conditions of 298 K and 1 atmosphere), R the universal gas constant, and T the absolute temperature. *K* is defined as

$$K = \prod a_i^{\upsilon_i} \tag{3}$$

where a_i represents the activity of the *i*th component in the reaction.

For equation (1), ΔG may also be expressed as Faraday's Law

$$\Delta G = -z\ F\ E_{rev} \tag{4}$$

in which z is the number of electrons transferred in the reaction, F the Faraday constant, and E_{rev} the reversible or equilibrium potential of the reaction in equation (1)

Under standard conditions

$$\Delta G^0 = -z\ FE^0 \tag{5}$$

where E^0 represents the standard potential of the reaction.

Combining equations (2), (4) and (5) yields an expression for the reversible potential of the reaction

$$E_{rev} = E^0 - \frac{RT}{zF} \ln K \tag{6}$$

Equation (1) may be written as

$$\sum \upsilon_{ox,i} B_{ox,i} + z\ e^- = \sum \upsilon_{red,i} B_{red,i} \tag{7}$$

in which $\upsilon_{ox,i}$ and $\upsilon_{red,i}$ represent the stoichiometric coefficients of the oxidized and reduced species $B_{ox,i}$ and $B_{red,i}$, respectively.

Equation (7) represents a cell reaction, made up of two electrode or half-cell reactions, an oxidation reaction and a reduction reaction. By convention, electrons appear on the left-hand side of the equation and both $\upsilon_{ox,i}$ and $\upsilon_{red,i}$ are always positive.

Therefore, for reaction (7), equation (6) may be written as

$$E_{rev} = E^0 - \frac{RT}{zF} \ln \left[\frac{\prod a_{red,i}^{\upsilon_{red,i}}}{\prod a_{ox,i}^{\upsilon_{ox,i}}} \right] \tag{8}$$

Equation (8) is known as the Nernst equation and permits the calculation of the potential of the reaction (E_{rev}) as a function of activity (a) and temperature (T). From equation (4) it is clear that, for a spontaneous reaction, $E_{rev} > 0$.

For practical purposes, the activity (a_i) may be replaced by the concentration (c_i) (15), thus

$$E_{rev} = E^0 - \frac{RT}{zF} \ln \left[\frac{\prod c_{red,i}^{\upsilon_{red,i}}}{\prod c_{ox,i}^{\upsilon_{ox,i}}} \right] \tag{9}$$

Published values of standard potentials (E^0), also known as standard reduction or half-cell potentials, are, by convention, measured with respect to the standard hydrogen electrode which is defined as $E^0 = 0$. As an example, consider the reaction

$$Zn^{++} + H_2 \rightleftharpoons 2H^+ + Zn \quad E^O = -0.76v \tag{10}$$

By convention, the half-cell reaction for the reduction of Zn^{++} is written as

$$Zn^{++} + 2e^- \rightleftharpoons Zn \quad E^0 = -0.76v \tag{11}$$

and the oxidation of molecular hydrogen to solvated protons is assumed.

Also by convention, the activity of solid substances is taken as unity and, therefore, the Nernst equation for equation (11) may be written as

$$E_{(Zn^{++}/Zn)} = -0.76 - \frac{RT}{2F} \ln \left[\frac{1}{c_{Zn^{++}}} \right] \tag{12}$$

By setting the ion concentration equal to 1 mol, the logarithmic term vanishes to give the measured potential $\left(E_{(Zn^{++}/Zn)}\right)$ equal to E^0.

In this paper, values of E^0 have been calculated from thermodynamic data for ΔG^0 collated by Bard, Parsons, and Jordan (16) and the application of Faraday's Law, equation (5). These calculated standard reduction potentials and the Nernst equation will be used to assist in explaining the experimental results obtained.

Experimental Details

Materials

Examples of the 10 metal elements and 10 alloys were obtained in sheet form from a variety of sources within the U.K., with Table 1 showing the elements and alloys used in these experiments, their source, and the composition of the alloys. Samples were prepared by cutting ~30 mm square pieces from each sheet. The thickness of the sheet varied between each metal, but was typically ~1 mm other than for gold, which was ~0.1 mm thick, and gold alloy which was ~0.2 mm thick.

Methods

Prior to any fingerprint deposition, all samples were washed in 0.5 L of warm water containing a few (3–4) drops of a commercial detergent (containing both anionic and nonionic surfactants). Following this, all samples were washed in distilled water, acetone, and then again in distilled water. Finally, each sample was dried with a paper towel. Fingerprints were deposited by pressing a finger onto the metal surface for 1–2 sec with a light pressure sufficient to ensure contact between the finger and metal. Whilst no attempt was made to regulate the amount of pressure applied by individuals, this procedure was intended to produce reasonably uniform deposition. All fingerprint donors washed their hands with soap and water 20 min prior to depositing fingerprints and no artificial stimulation of sweat was employed, such as placing the hand in a plastic bag (17) or wearing a latex glove prior to deposition (18). To evenly distribute sweat, donors rubbed their hands together prior to deposition.

All samples were left in air at room temperature (18 ± 5°C) for a period of 10 days, this time period being in keeping with our previous work (11). After the 10-day period, samples were washed in a solution of warm water containing a few drops of the commercial

detergent used to initially clean the disks. The disks were rubbed vigorously with a nonabrasive cloth to remove all traces of fingerprint residue. Each sample was then assessed as to the degree of corrosion of the metal by the fingerprint residue using the grading system devised by Bandey (19), which is reproduced in Table 2.

Results and Discussion

Metal Elements

Forty donors provided a fingerprint from a different finger on each of the 10 metal elements listed in Table 1 above, providing 400 donations in total. A different finger was used for each donation to ensure that the amount of sweat deposited did not reduce, as would have happened if the same finger had been used repeatedly on different elements. Ten days after the deposition, all samples were washed as described above and graded according to Table 2. As was observed in our previous work (11), there was a range of fingerprint ridge detail development, Fig. 1 showing the percentage of samples for each element that produced either a grade 3 or 4 development.

Figure 1 shows the elements in order of increasing standard reduction potential, that is, the most reactive (least noble) elements are shown on the left and the least reactive (most noble) elements on the right. The four most reactive elements (magnesium, aluminum, titanium, and zinc) produced no grade 3 or 4 ridge development. In fact, none of these elements produced any ridge development and were all graded at 0. This is in keeping with our previous results for aluminum (11). While it might be expected that these elements would produce a corrosive reaction with fingerprint residue, it is well known that their low reduction potentials (relative to the more noble elements) favor the growth of passive oxide films on the surface of the metal through the reduction of oxygen in moist air (20).

If thermodynamically favorable, the reduction of oxygen causes spontaneous passivation (chemical passivation) of the metal and the cell potential can be expressed in terms of each of the two half-cell reactions (the reduction and the oxidation half-cells) as

$$E_{rev} = E_{red} + E_{ox(metal)} > 0 \quad (13)$$

The metal oxidation is represented by $E_{ox\ (metal)}$ which is equivalent to $-(E_{red(metal)})$. Therefore, rearranging equation (13) gives

$$E_{red} > E_{red(metal)} \quad (14)$$

Thus, metals with reduction potentials less than the reduction potential of the reduction half-cell will tend to passivate spontaneously. A passivating potential (E_p) can be defined for the metal anodic reaction, which specifies the potential above which the metal is considered passivated. Successful spontaneous and stable passivation requires $E_p < E_{red}$ (21).

Elements with higher standard reduction potentials produced a number of grade 3 or 4 ridge detail development and the results for copper are consistent with our previous work (11). Examples of full ridge detail development are shown in Fig. 2 for nickel, tin, copper, silver, and gold, respectively. It is perhaps surprising that noble elements (silver and gold) produced grade 3 or 4 developments, both silver and gold producing similar percentages to nickel, tin, and lead.

An explanation for this behavior lies in the formation of complex metal ions in the aqueous solution of the fingerprint residue. It is well known that a metal dissolving in the presence of a suitable complexing agent will form a complex ion with a decrease in the reduction potential, that is, the metal ion complex is less noble than the metal (13). For both silver and gold, the presence of chloride ions in the fingerprint residue enable complex metal chloride ions to be formed.

TABLE 1—*The elements and alloys used in these experiments their source and the composition of the alloys.*

Name	Composition	Supplier
Aluminum	Impurities <0.001%	Nobles Engineering Solutions, Northampton, U.K.
Aluminum (alloy) LM6	A casting alloy with the addition of Si(~12%), <1% of Fe, Mn, Cu, Zn, Ni, Mg, Pb, Sn, Ti	Dyson Diecasting Ltd, Bletchley, U.K.
Aluminum (alloy) LM24	A casting alloy with the addition of Si(~8%), Cu(~3%), Zn(3%), Fe(~1%), <1% of Mg, Mn, Ni, Pb, Sn, Ti	Dyson Diecasting Ltd, Bletchley, U.K.
Brass	Yellow brass, Cu(67%), Zn(33%)	Nobles Engineering Solutions, Northampton, U.K.
Copper	Impurities <0.0001%	Nobles Engineering Solutions, Northampton, U.K.
Gold	24 Karat	Organique Designer Jewellery, Wellingborough, U.K.
Gold (alloy)	9 Karat, Cu(42%), Ag(~17%), Zn(3%).	Organique Designer Jewellery, Wellingborough, U.K.
Lead	Impurities <0.001%	British Lead Mills, Welwyn Garden City, U.K.
Magnesium	Impurities <0.001%	Super Alloys International Ltd, Milton Keynes, U.K.
Nickel	Impurities <0.01%	Super Alloys International Ltd, Milton Keynes, U.K.
Nickel (alloy) C263	A nickel Hastelloy with the addition of Cr(20%), Co(~19%), Mo(~6%), Ti(~2%), <1% C, Mn, Fe, Si, Cu, Al	Super Alloys International Ltd, Milton Keynes, U.K.
Nickel silver NS106	Comprising Cu(63%), Ni(18%), Zn(~18%), <1% Mn	Knight Strip Metals Ltd, Potters Bar, U.K.
Silver	Impurities <0.01%	Organique Designer Jewellery, Wellingborough, U.K.
Silver (alloy)	Sterling silver Cu(7.5%)	Organique Designer Jewellery, Wellingborough, U.K.
Steel (alloy) 4130	Addition of <1% of various alloying elements, C, Mn, A1, Si, Cu, Ni, Cr, Mo	Super Alloys International Ltd, Milton Keynes, U.K.
Steel (stainless) 316	An Austenitic steel with the addition of Cr(~17%), Ni(~10%), Mo(~2%), Mn(~2%), <1% of C, N, Si, P, Co	Super Alloys International Ltd, Milton Keynes, U.K.
Steel EN8	Medium carbon steel, addition of <1% of various alloying elements, C, Si, Mn, S, P	Nobles Engineering Solutions, Northampton, U.K.
Tin	Impurities <0.01%	Blue Hills Tin Streams, St Agnes, U.K.
Titanium	Commercially pure grade 1	Super Alloys International Ltd, Milton Keynes, U.K.
Zinc	Impurities <0.01%	Dyson Diecasting Ltd, Bletchley, U.K.

TABLE 2—*Grading system for determining the quality of ridge detail for enhanced fingerprints devised by Bandey (19).*

Grade	Comments
0	No development
1	Absent continuous ridges. All discontinuous or dot like
2	One-third of mark continuous ridges (Remaining no development)
3	Two-thirds of mark continuous ridges (Remaining no development)
4	Full development. Whole fingerprint continuous ridges

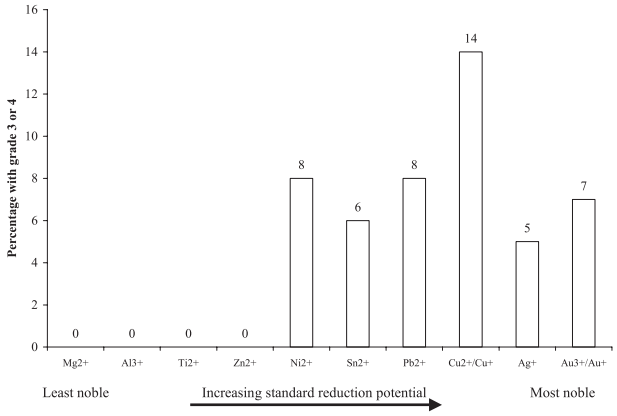

FIG. 1—*Percentage of each element that produced either a grade 3 or 4 fingerprint ridge detail development. The elements are shown in order of increasing standard reduction potential (13).*

Consider the reaction for gold

$$4Au + 8[Cl^-] + 2H_2O + O_2 \rightleftharpoons 4[AuCl_2]^- + 4[OH]^- \qquad (15)$$

In the presence of water and dissolved oxygen (constituents of fingerprint residue) the monovalent gold complex $[AuCl_2]^-$ can form. The half-cell reaction

$$[AuCl_2]^- + e^- \rightleftharpoons Au + 2[Cl^-] \qquad (16)$$

yields $E^0_{comp} = 1.15v$, compared with $E^0 = 1.83v$ for the half-cell reaction.

$$Au^+ + e^- \rightleftharpoons Au \qquad (17)$$

Trivalent gold is generally more stable than monovalent gold (13) and the equivalent trivalent complex $[AuCl_4]^-$ has $E^0_{comp} = 1v$.

It must be emphasized at this point that quoted values for E^0 and E^0_{comp} are based on ion concentrations of 1 mol and, therefore, are indicative only of the trend of reduction potentials rather than actual values for the reactions being considered. Nevertheless, the presence of chloride ions in the fingerprint residue offers an explanation for the experimental observations with gold.

By applying the Nernst equation to equations (16) and (17), it is possible to calculate the ratio of the complex ion activity (concentration) to the product of the reactant ion activities (concentrations). This ratio is known as the complexation constant κ (13). For the complexation reaction

$$Au^+ + 2\ Cl^- \rightleftharpoons [AuCl_2]^- \qquad (18)$$

κ is defined as

$$\kappa = \frac{a_{[AuCl_2]^-}}{a_{Au^+} \cdot a^2_{Cl^-}} \qquad (19)$$

The complexation reaction (16) gives a Nernst equation of

$$E_{comp} = E^0_{comp} - \frac{RT}{zF} \ln\left[\frac{a^2_{Cl^-}}{a_{[AuCl_2]^-}}\right] \qquad (20)$$

and the half-cell reaction (17) gives

$$E_{rev} = E^0 - \frac{RT}{zF} \ln\left[\frac{1}{a_{Au^+}}\right] = E^0 - \frac{RT}{zF} \ln\left[\frac{\kappa \cdot a^2_{Cl^-}}{a_{[AuCl_2]^-}}\right] \qquad (21)$$

As stated above, at equilibrium $\Delta G = 0$ and so re-arranging equations (20) and (21) yields

$$E^0_{comp} = E^0 - \frac{RT}{zF} \ln[\kappa] \qquad (22)$$

Thus, equation (22) gives the complexation constant in terms of the standard reduction potentials of equations (16) and (17). A standard temperature of 298 K and calculated values for both E^0_{comp} (equation 16) and E^0 (equation 17) gives a value for κ of $\sim 10^{11}$ mol^{-2} L^2. Thus, in the presence of chloride ions, the concentration of complex $[AuCl_2]^-$ ions is many orders of magnitude greater than the concentration of monovalent gold ions leading to a corresponding reduction in the standard potential and hence gold behaving less like a noble metal.

For the trivalent gold complexation reaction with chloride ions

$$[AuCl_4]^- + 3e^- \rightleftharpoons Au + 4\ Cl^- \qquad (23)$$

the equivalent values for E^0 and E^0_{comp} are $1.52v$ and $1v$, respectively, giving a value of $\kappa \sim 10^{26}$ mol^{-4} L^4.

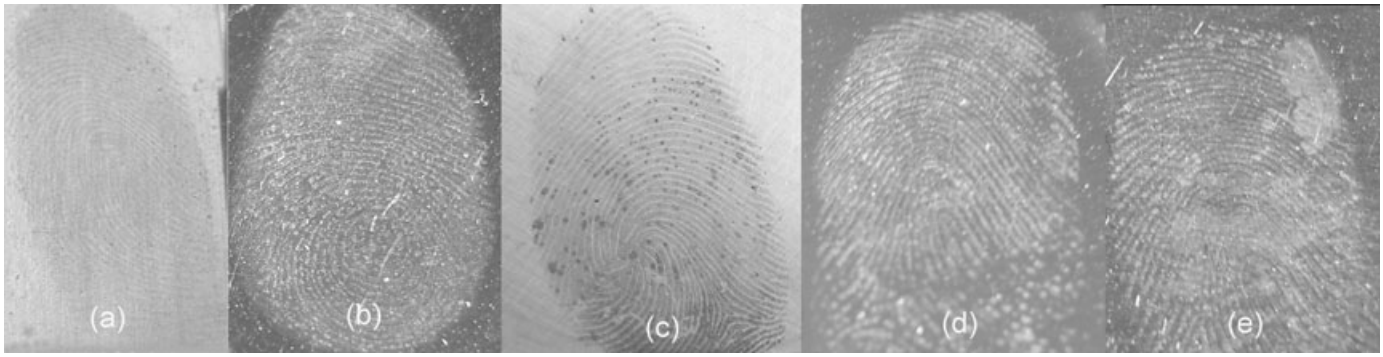

FIG. 2—*Typical full ridge detail development for (a) nickel, (b) tin, (c) copper, (d) silver, and (e) gold. All samples were washed 10 days after fingerprint deposition.*

Silver will form monovalent chloride complexes similar to gold and replacing gold with silver in equations (16) and (17) gives $E^0 = 0.8v$, $E^0_{comp} = 0.48v$ and $\kappa = \sim 10^5$ mol^{-2} L^2. The lower value of κ compared with monovalent gold might explain why silver produced less grade 3 or 4 ridge detail development than gold. Another possible explanation is the lowering of the chloride ion concentration through the precipitation of the sparingly soluble salt, AgCl. Application of the Nernst equation to the half-cell reaction

$$[AgCl_2]^- + e^- \rightleftharpoons Ag + 2[Cl^-] \quad (24)$$

shows that, as the concentration of Cl^- reduces, E_{comp} increases reducing the effect of the complexation.

Other (lower reduction potential) elements considered in this study will also form metal ion complexes, such as $[CuCl_2]^-$, which has $E^0 = 0.52\ v$, $E^0_{comp} = 0.23\ v$ and $\kappa = 10^5$ mol^{-2} L^2. However, as these elements are less noble than silver or gold, the explanation for the observed corrosion with fingerprint residue is less dependent on the formation of metal halide complexes.

Metal Elements—Cleaned Abrasively

We considered next the effect that removing any oxide layer from the metal would have on corrosion by fingerprint residue. Forty fresh samples of each of the 10 elements were prepared by cleaning abrasively with grade 000 steel wool. Each sample was then washed following the method described above for the initial samples. The same 40 donors then provided a fingerprint from a different finger on each of the 10 metal elements providing an additional 400 donations in total. Ten days after the deposition, all samples were washed as previously described and graded according to Table 2. Figure 3 shows the percentage of samples for each element that produced either a grade 3 or 4 development.

Figure 3 shows that, with the exception of titanium, those elements that failed previously to produce any grade 3 or 4 development above (magnesium, aluminum, and zinc) produced the highest percentages after cleaning abrasively. Other elements that previously produced some grade 3 or 4 development, with the exception of gold, showed an increase in the percentage after cleaning abrasively. Ignoring titanium, silver, and gold for the moment, the increase observed with these other elements can be explained by spontaneous passivation as described in equations (13) and (14) above. The half-cell reduction reaction for water and dissolved oxygen

$$O_2 + 2H_2O + 4e^- \rightleftharpoons 4[OH]^- \quad (25)$$

has $E^0 = 0.4$ v. Therefore, spontaneous passivation is thermodynamically favorable for elements with $E^0 < 0.4v$. This includes all of those elements for which an increase in grade 3 or 4 development was observed. Thus, irrespective of the chloride ion concentration in the fingerprint residue, equation (25) provides a mechanism for the water content of the residue and dissolved oxygen to corrode the metal. For silver and gold, $E^0 >> 0.4v$, which would explain why cleaning abrasively had little effect on the development for gold. For silver, the small increase may be due to the formation of a silver chloride complex because, as stated above, $E^0_{comp} = 0.48v$ which is $\approx E^0$ for the half-cell reduction reaction (25), remembering that these values for E^0 are indicative only as they are based on ion concentrations of 1 mol.

The experimental results for titanium appear anomalous in that its standard reduction potential would imply a degree of corrosion equitable with other elements near to it in the reduction table (magnesium, aluminum and zinc). However, it is well known that, if removed, the passivating oxide layer on titanium immediately reforms if the metal surface is exposed to moist air, the surface film thickness quickly reaching ~1 nm (22).

Figure 4 shows typical full development of fingerprint ridge detail for magnesium, zinc, and aluminum, respectively.

Abrasive cleaning was found to improve the ease with which fingerprint corrosion could be visualized in some elements when compared with samples cleaned nonabrasively, Fig. 5 showing a typical example for lead.

It is worth noting that the ridge detail developed following abrasive cleaning of the metal disappeared slowly on lower reduction potential elements as the metal once again oxidized in air. On magnesium the developed fingerprints were obliterated completely several weeks after cleaning.

Metal Alloys

The same 40 donors provided a fingerprint from a different finger on each of the 10 metal alloys listed in Table 1 above, providing a further 400 donations in total. Ten days after the deposition, all samples were washed as described above and graded according to Table 2, Fig. 6 showing the percentage of samples for each alloy

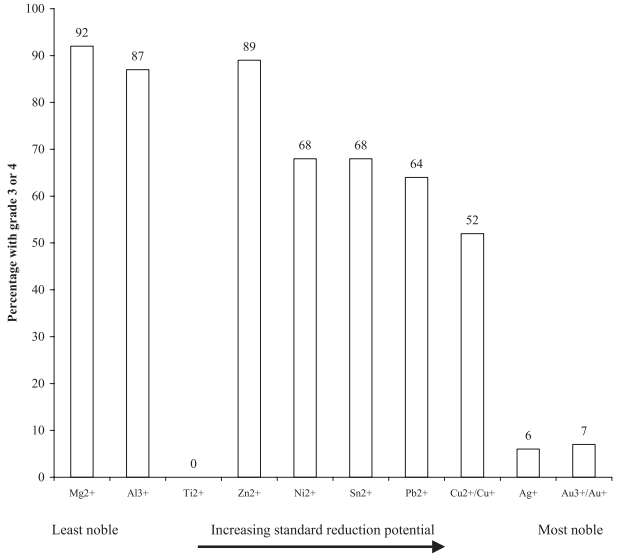

FIG. 3—*Percentage of each element cleaned abrasively that produced either a grade 3 or 4 fingerprint ridge detail development. The elements are shown in order of increasing standard reduction potential (13).*

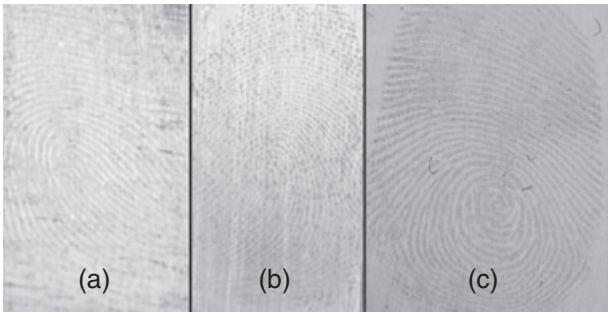

FIG. 4—*Typical full ridge detail development for (a) magnesium, (b) zinc, and (c) aluminum. All samples were cleaned abrasively and then washed 10 days after fingerprint deposition.*

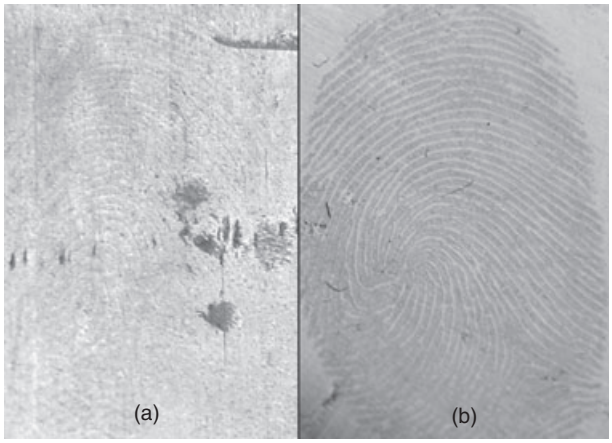

FIG. 5—*Typical full ridge detail development for lead with sample (a) cleaned nonabrasively and (b) cleaned abrasively. Both samples were washed 10 days after fingerprint deposition.*

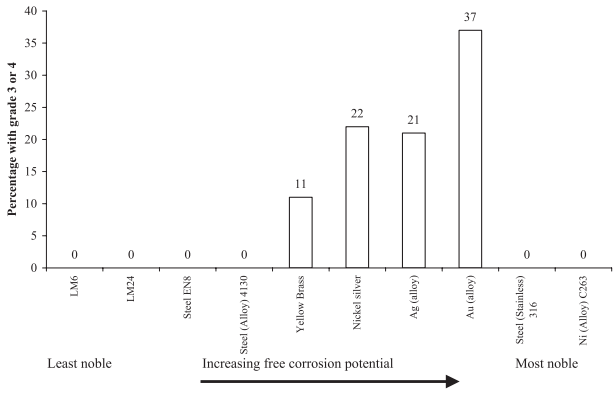

FIG. 6—*Percentage of each alloy that produced either a grade 3 or 4 fingerprint ridge detail development. The alloys are shown in order of increasing free corrosion potential (14).*

that produced either a grade 3 or 4 development. In Fig. 6 the alloys are listed in the order of a galvanic series, recorded at 25°C in seawater (14). A galvanic series is an experimental ordering of metals (elements and alloys) based on their free corrosion potential, which is dependent on environmental conditions, such as temperature, pressure, and electrolyte and, therefore, the relative position of a metal in the series may shift as environmental conditions change. Equally, a given metal may appear twice in the same series in both a passivated and active state. Being a kinetic quantity, corrosion potential is different to reduction potential, which is based on thermodynamic properties.

Of the alloys that produced no grade 3 or 4 development, the aluminum alloys (LM6 and LM24) both contain silicon, which is well known to give excellent corrosion resistance (23). Stainless steel (316) and nickel alloy (C263) are both passivated by the addition of high percentages of chromium, whilst the low alloy steel (4130) and the medium carbon steel (EN8) also produced no grade 3 or 4 development.

Of those alloys that did produce some grade 3 or 4 development, brass gave results in keeping with our previous work (11) and the corrosion may be due to dezincification, which is well known to occur in brass containing >15% zinc in the presence of chloride ions (23). Nickel silver, containing 63% copper, showed grade 3 or 4 development in nearly a quarter of the samples. Silver alloy (containing ~7.5% copper) produced a higher percentage of grade 3 or 4 development than elemental silver (Fig. 1) with, clearly, the addition of the alloying copper affecting the corrosion. The biggest difference between grade 3 or 4 development for an element and its alloy occurred with gold. 9 Karat gold alloy, comprising 62% alloying elements of mainly copper (42%) and silver (17%), produced grade 3 or 4 development for 37% of samples. It is well known that gold-copper alloys can exhibit selective corrosion of copper (21). Clearly, the inclusion of more reactive (lower reduction potential) elements, such as copper, provide a suitable environment for corrosion of alloys by fingerprint residue. Corrosion of these alloys was found to permit an easier visualization of the fingerprint corrosion through enhanced contrast between the corroded and un-corroded metal. Such enhanced contrast was noted for all three alloys containing a large (> ~40%) percentage of copper. This property of fingerprint corrosion on metal alloys is considered again later in this paper.

Examples of full ridge detail development for nickel silver, silver alloy, and gold alloy are shown in Fig. 7.

Metal Alloys—Cleaned Abrasively

In a similar fashion to the metal elements, the 10 metal alloys were cleaned abrasively and washed to remove any oxide layer from the metal surface. It was noticed that the grade of steel wool used (000) did not appear to effectively remove the chromium oxide layer from the passivated stainless steel (316) and nickel alloy (C263) and

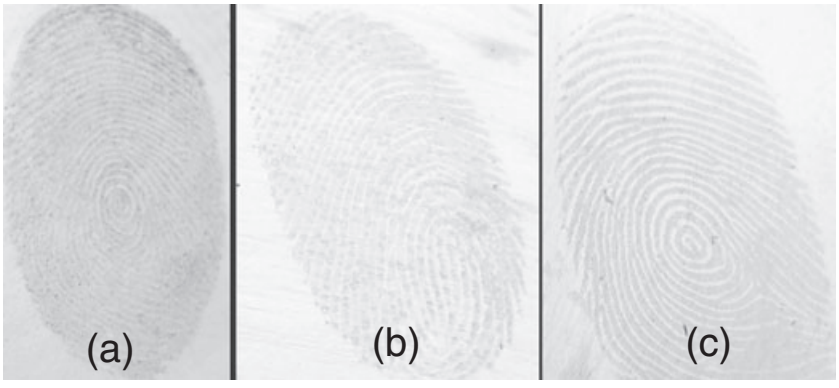

FIG. 7—*Typical full ridge detail development for (a) nickel silver, (b) silver alloy, and (c) gold alloy. All samples were washed 10 days after fingerprint deposition.*

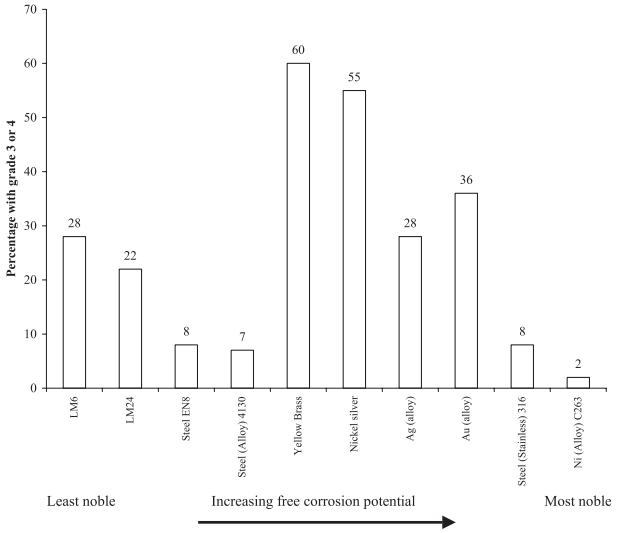

FIG. 8—*Percentage of each alloy cleaned abrasively that produced either a grade 3 or 4 fingerprint ridge detail development. The alloys are shown in order of increasing free corrosion potential (14).*

therefore a coarser grade of steel wool (grade 0) was used on these two alloys. A further set of 400 fingerprint deposits were then taken from the same 40 donors. Ten days after the deposition, all samples were washed as described above and graded according to Table 2, Fig. 8 showing the grade 3 or 4 results.

From Fig. 8, the most notable change in the percentage of grade 3 or 4 development compared with Fig. 6 (alloys cleaned nonabrasively) occurred for brass and nickel silver with changes from 11% to 60% and 22% to 55%, respectively. Clearly, the removal of the oxide layer on the surface of these alloys permits greater corrosion by the fingerprint residue whereas for both silver and gold alloys, the abrasive cleaning produced no increase in grade 3 or 4 development. The aluminum, steel, and nickel alloys all produced non zero results with the aluminum alloys giving grade 3 for 4 development in ~25% of samples despite the inclusion of silicon in these casting alloys. The steel and nickel alloys produced lower results (<10%) although similar results for all three steel alloys would suggest that effective removal of the passivating layer from stainless steel (316) had been achieved by the coarser steel wool.

Figure 9 shows typical full ridge detail development for alloys that produced nonzero grade 3 or 4 development after abrasive cleaning.

In a similar fashion to Figs. 5 and 10 shows the improved visualization of fingerprint corrosion on brass resulting from abrasive cleaning of the alloy.

Fingerprint Corrosion Series

We now present in Table 3 results from the above experimental data as a fingerprint corrosion series for the 10 elements and 10 alloys, both cleaned abrasively and nonabrasively. The metals are shown in order of increasing fingerprint corrosion (from top to bottom) and the diamond shape in each row indicates the percentage of grade 3 or 4 development for that metal.

Fingerprint Visualization on Metal Alloys

We noted above that the fingerprint corrosion of alloys containing a large percentage of copper (brass, gold alloy, and nickel silver) was visualized easily through enhanced contrast between the corroded and noncorroded alloy. This effect was found to be most noticeable on gold alloy, through selective corrosion of the copper (21), where it was observed that the contrast permitted fine detail and third level fingerprint characteristics to be observed. Third level fingerprint characteristics include small shapes on the ridge (edgeoscopy), ridge width and relative pore location (poroscopy), collectively known as ridgeology (24). If such a level of fine detail is required for a fingerprint comparison, the fingerprints of a suspect would be taken either conventionally as inked impressions on paper or digitally by the donor placing their hand on a glass platen through which their fingerprints would be captured electronically and then printed, a technique known as Livescan. Satisfactory results require the correct pressure to be exerted on the donor's finger whilst the former method also requires an appropriate amount of ink to be used, so as not to obliterate the fine detail. It occurred to us that taking a donor's fingerprints on gold alloy might consistently produce a more defined pattern of third level characteristics than either of the above mentioned methods. To test this, we took an additional sample of fingerprints from 40 donors by the conventional inking method, Livescan and on gold alloy. This produced 120 fingerprints in total, 40 by each of the three capture methods. The fingerprints of each donor (ink, Livescan and gold alloy) were taken by a different operator, trained to take fingerprint impressions. We found that third level detail on conventional inked impressions was easily, and frequently, obliterated by over or under inking or by too little or too much pressure being exerted on the donor's finger. Such pressure variation by the operator also readily obliterated this detail with Livescan impressions. After 10 days, the 40 gold alloy depositions were washed in the usual manner prior to assessment. Fourteen samples gave a grade 3 or 4 development, all of which displayed third level detail. For eight of the 14 samples, the gold alloy fingerprint displayed more third level detail than the inked or Livescan equivalent, Fig. 11 showing a typical example.

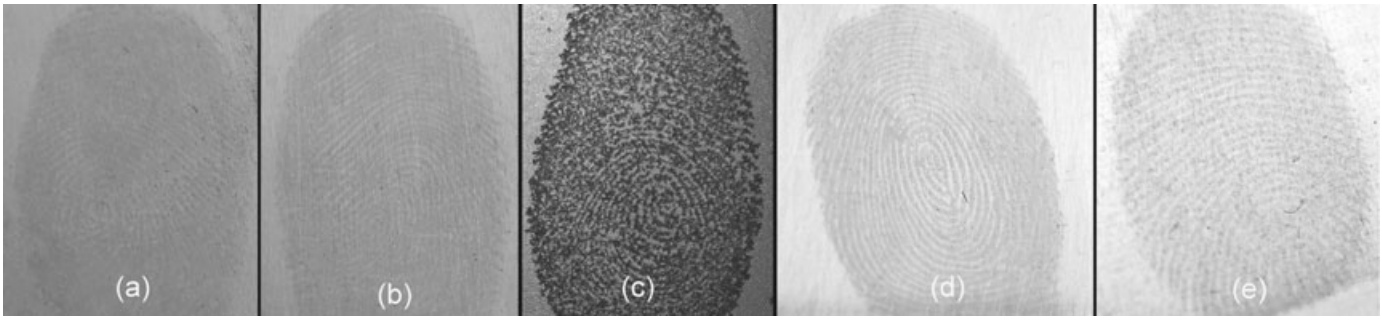

FIG. 9—*Typical full ridge detail development for (a) aluminum alloy (LM6), (b) aluminum alloy (LM24), (c) steel (EN8), (d) stainless steel (316), and (e) nickel alloy (C263). All samples were cleaned abrasively and then washed 10 days after fingerprint deposition.*

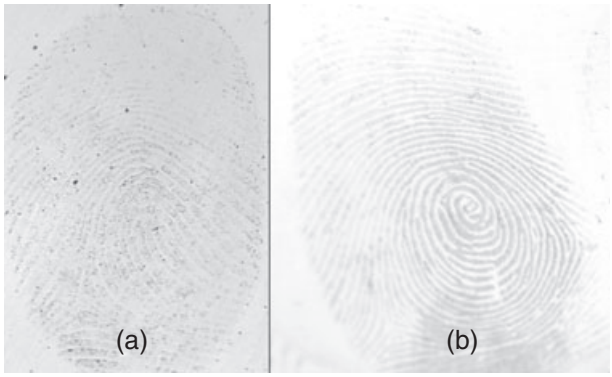

FIG. 10—*Typical full ridge detail development for brass with sample (a) cleaned nonabrasively and (b) cleaned abrasively. Both samples were washed 10 days after fingerprint deposition.*

While the overwhelming majority of fingerprint identifications are made using second level detail (ridge characteristics), the deposition of fingerprints on metal alloys offers an alternative means of capturing third level detail when required for a fingerprint comparison.

Conclusions

This current study has investigated further fingerprint corrosion of metals by broadening the range of metals examined to include 10 metal elements and 10 metal alloys. Elements and alloys were prepared by both abrasive and nonabrasive cleaning, the former intended to remove any passivating coating present on the metal surface.

Likely oxidation/reduction reactions taking place between the 10 different elements and fingerprint residue have been considered in terms of both the reduction potential of the elements and the degree of corrosion observed. By applying the Nernst equation, calculated values for the standard reduction potential (E^0) and complexation constant (κ) have been used to provide a thermodynamic explanation for the experimental results. The corrosion of noble metals, such as silver and gold, has been presented as further evidence to support our previous studies, which found that metal corrosion is enhanced by the presence of aggressive ions (such as chloride) in eccrine sweat.

Also, this work has highlighted again the variation in both the amount and composition of eccrine sweat secreted by different donors and, although not pursued in this study, is still a subject for further investigation, not least because the concentration of aggressive ions, such as chloride, would appear to be crucial for the success of fingerprint enhancement techniques that require corrosion of the metal surface.

Experiments on 10 different metal alloys (also cleaned abrasively and nonabrasively) permitted the construction of a fingerprint corrosion series for both the elements and alloys.

Observed results for the alloys revealed that elements alloyed with > ~40% copper produced the highest degree of alloy corrosion by fingerprint residue and these alloys produced an image of the fingerprint that included third level fingerprint detail, such as pores, and their relative location. This property was found to be

TABLE 3—*Fingerprint corrosion series for the 10 elements and alloys.*

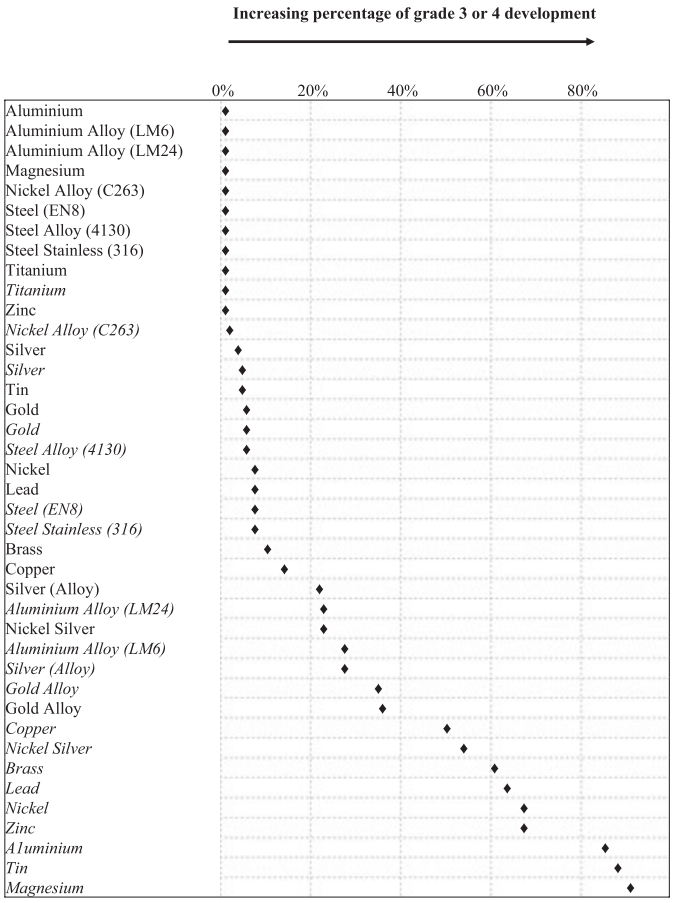

Names shown in normal font indicate nonabrasive cleaning of the metal whilst italics indicate abrasive cleaning.

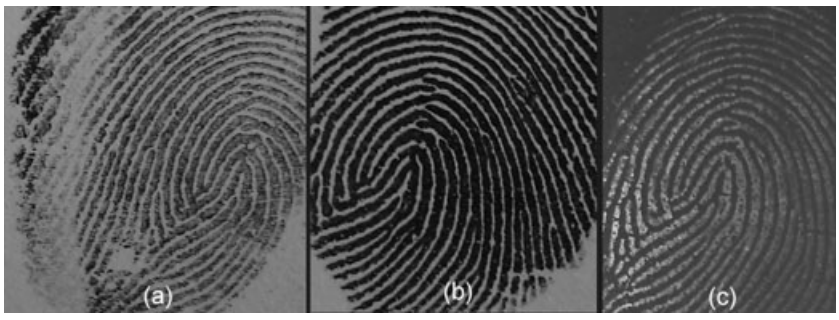

FIG. 11—*Typical example of a fingerprint from the same donor and taken by the same operator by (a) livescan, (b) ink on paper, and (c) sweat deposit on gold alloy. Sample (c) was left for 10 days after deposition before assessment.*

most acute on 9 Karat gold alloy and a comparison with both conventional inked and digital (Livescan) fingerprints showed that fingerprints deposited on gold alloy were least susceptible to the obliteration of third level detail. Whilst examination of third level detail is not the most common means of fingerprint comparison, it can prove useful if present in both the known exemplar and unknown prints. We feel that this property of gold alloy is worthy of further experimentation.

Work is currently being undertaken to further investigate both the physical and chemical changes taking place at the surface of a metal as a result of fingerprint residue corrosion. Work is also underway to measure anion and cation concentrations in eccrine sweat, their variation between individuals and how this affects metal corrosion by fingerprint residue.

Acknowledgments

The author is indebted to the many members of Northamptonshire Police who, over an extended period, willingly donated their latent fingerprints for this research. The assistance of Mrs. Trudy Loe, Research Assistant with Northamptonshire Police, with the preparation of the manuscript is acknowledged with thanks. The support of the Chief Officers of Northamptonshire Police in enabling this research to have been conducted is gratefully acknowledged.

References

1. Trethewey KR, Chamberlain J. Corrosion for science and engineering. Harlow, England: Longman Scientific, 1995;1–22.
2. Czekanski P, Fasola M, Allison J. A mechanistic model for the superglue fuming of latent fingerprints. J Forensic Sci 2006;51:1323–8.
3. Bowman V, editor. Manual of fingerprint development techniques. 2nd rev. ed. Sandridge, UK: Police Scientific Development Branch, Home Office, 2004.
4. Bandey H, Kent T. Superglue treatment of crime scenes. Sandridge, UK: Police Scientific Development Branch, Home Office, 2003 Report No: 30/03.
5. Bersellini C, Garofano L, Giannetto M, Lusardi F, Mori G. Development of latent fingerprints on metallic surfaces using electropolymerization processes. J Forensic Sci 2001;46:871–7.
6. Cantu AA, Leben DA, Ramotowski R, Kopera J, Simms JR. Use of acidified hydrogen peroxide to remove excess gun blue-treated cartridge cases and to develop latent prints on untreated cartridge cases. J Forensic Sci 1998;43:294–8.
7. Smith K, Kauffman C. Enhancement of latent prints on metal surfaces. J Forensic Ident 2001;51:9–15.
8. Migron Y, Mandler D. Development of latent fingerprints on unfired cartridges by palladium deposition: a surface study. J Forensic Sci 1997;42:986–92.
9. Williams G, McMurray HN, Worsley DA. Latent fingerprint detection using a scanning Kelvin microprobe. J Forensic Sci 2001;46:1085–92.
10. Williams G, McMurray N. Latent fingermark visualization using a scanning Kelvin probe. Forensic Sci Int 2007;167:102–9.
11. Bond JW. Visualization of latent fingerprint corrosion of metallic surfaces. J Forensic Sci 2008;53:812–22.
12. Lee HC, Gaensslen RE. Methods of latent fingerprint development. In: Lee HC, Gaensslen RE, editors. Advances in fingerprint technology. New York: Elsevier, 2001;63–104.
13. Landolt D. Corrosion and surface chemistry of metals. Lausanne, Switzerland: CRC Press, 2007;15–58.
14. Trethewey KR, Chamberlain J. Corrosion for science and engineering. Harlow, England: Longman Scientific, 1995;69–143.
15. Housecroft CE, Sharpe AG. Inorganic chemistry. Harlow, England: Pearson, 2005;162–91.
16. Bard AJ, Parsons R, Jordan J, editors. Standard potentials in aqueous solution. New York: Marcel Dekker, 1985.
17. Migron Y, Hocherman G, Springer E, Almog J, Mandler D. Visualization of sebaceous fingerprints on fired cartridge cases: a laboratory study. J Forensic Sci 1998;43:543–8.
18. Worley CG, Wiltshire SS, Miller TC, Havrilla GJ, Majidi V. Detection of visible and latent fingerprints using micro-x-ray fluorescence elemental imaging. J Forensic Sci 2006;51:57–63.
19. Bandey HL. Fingerprint development and imaging newsletter: the powders process, study 1. Sandridge: Police Scientific Development Branch, Home Office, 2004 Report No: 54/04.
20. Trethewey KR, Chamberlain J. Corrosion for science and engineering. Harlow, England: Longman Scientific, 1995;406–26.
21. Landolt D. Corrosion and surface chemistry of metals. Lausanne, Switzerland: CRC Press, 2007;227–329.
22. Titanium Metals Corporation. Technical Manual. Corrosion resistance of titanium. Denver: Titanium Metals Corporation, 1997. Available at: http://www.timet.com/index_new.htm. Accessed July 30, 2008.
23. Trethewey KR, Chamberlain J. Corrosion for science and engineering. Harlow, England: Longman Scientific, 1995;336–74.
24. Ashbaugh DR. Quantitative-qualitative friction ridge analysis. Boca Raton: CRC Press, 1999.

Additional information and reprint requests:
John W. Bond, D.Phil.
Scientific Support Unit
Northamptonshire Police
Wootton Hall
Northampton NN4 OJQ, U.K.
E-mail: john.bond@northants.police.uk